ARTICLE IN PRESS

Available online at www.sciencedirect.com

ScienceDirect

journal homepage: http://www.elsevier.com/locate/acme

ELSEVIER

ARCHIVES
OF CIVIL AND MECHANICAL
ENGINEERING

Original Research Article

Sensitivity and reliability analyses of lateral-torsional buckling resistance of steel beams

Z. Kala [*]

Brno University of Technology, Faculty of Civil Engineering, Department of Structural Mechanics, Veveří Street 95, 602 00 Brno, Czech Republic

ARTICLE INFO

ABSTRACT

The presented paper deals with an analysis of the effects of random imperfections on the load carrying capacity of a steel beam, which is subjected to the effects of lateral-torsional buckling arising from equal and opposite end bending moments. The load carrying capacity of a hot-rolled steel beam was analyzed in the analytical form. Histograms obtained from experimental research were available for most imperfections. Realizations of the input imperfections were computed using the Latin Hypercube Sampling method. Global sensitivity analysis was used to identify those imperfections, whose variability has a dominant effect on the load carrying capacity. Sensitivity analysis identified three continuous intervals of beam slenderness in which the load carrying capacity is sensitive to different types of imperfections. Reliability of design according to the EUROCODE 3 standard was verified by performing the statistical analysis of the ultimate limit state.

© 2015 Politechnika Wrocławska. Published by Elsevier Sp. z o.o. All rights reserved.

1. Introduction

I-beams are usually made of structural steel and are used in construction and civil engineering [1]. An I-shaped section is a very efficient form for carrying both bending and shear loads in the plane of the web, but has low carrying capacity in the plane associated with bending about its minor principal axis, and is furthermore inefficient in carrying torsion [1]. I-beams can thus be effectively used for carrying bending about their major principal axis. The load carrying capacity of an I-beam decreases with its increasing length (slenderness) due to lateral-torsional buckling (LTB).

The LTB behaviour of I-beams is very sensitive to imperfections [2,3]. The methods for modelling imperfections can be classified as deterministic or random [4]. Random uncertainty of imperfections can be taken into account in stochastic models using random variables or random fields [5,6]. The thesis [5] studies very similar subject matter as the presented paper, i.e. the effects of random imperfections on the stability of steel structures. The thesis [5] presents on a series of slender I-beams the simulation of buckling variability combining advanced methods of nonlinear structural shell finite elements and modern stochastic process theory. The greater the complexity of the stochastic model, the more information on input random imperfections is needed. At

2

present, in the case of frame structures, we can encounter problems focused on the modelling of initial geometric imperfection using linear combinations of eigenmodes [7]. Works aimed at the global sensitivity analysis of the influence of imperfections on limit states of structures occur rarely, although imperfections may drastically reduce the theoretical ultimate strength of perfect members.

The presented paper deals with the statistical and global sensitivity analyses of the LTB reliability of a simply supported hot-rolled steel European IPE 220 beam with initial random imperfections. The beam IPE 220 has an I-shaped cross-section, see Fig. 1 and [8–10]. Attainment of the limit state (in general, occurrence of failure) cannot, due to technical and economic reasons, be eliminated completely. Structures are therefore designed so that the probability of failure is minimal while the structure is still cost-effective. There are two types of structural limit states. One is pertinent to the load carrying capacity (ultimate limit state), and the other to serviceability (serviceability limit state). In the context of stability problems of steel structures, the load carrying capacity is generally more important than the structural serviceability, because it is related to ensuring the structure safety against collapse.

The load carrying capacity is generally a random variable that is dependent on input random material and geometric imperfections. The load carrying capacity is most frequently studied experimentally in a laboratory, while its random properties are studied using numerical, stochastic models and with the aid of computers. The reliability required for steel structures is obtained through design according to EN 1990 [11] and EN 1993 (EUROCODE 3) [12]. According to [11], the design load carrying capacity can be obtained as the lower quantile of the random load carrying capacity, see, e.g. [13,14,8]. EURO-CODE 3 lists the rule for evaluation of the design buckling resistance moment using characteristic values of material properties, nominal values of geometric characteristics, and partial safety factors. The design reliability according to [12] may be verified using the general principles for structural design of civil engineering works given in [11].

The derivation of the close-form formula for the elastic load carrying capacity of an imperfect IPE-beam loaded in bending is performed in this article. The analysis stems from the works of [15] and [16,17]. Imperfections are considered as random variables according to the results of experimental research [9,25]. The influence of random imperfections on the ultimate limit state of slender beams is studied using global sensitivity analysis (SA) [18] analogously as, e.g. in [19]. The imperfections, which have the greatest effect on reliability and should thus be addressed in experiments with the aim of the most precise determination of their random variability, were determined applying SA. The reliability of design according to [12] was verified using statistical analysis of the ultimate limit state. Non-dimensional beam slenderness $\bar{\lambda}_{LT}$ evaluated according to [12], enabling a more general comparison of results, was considered as the analysis parameter.
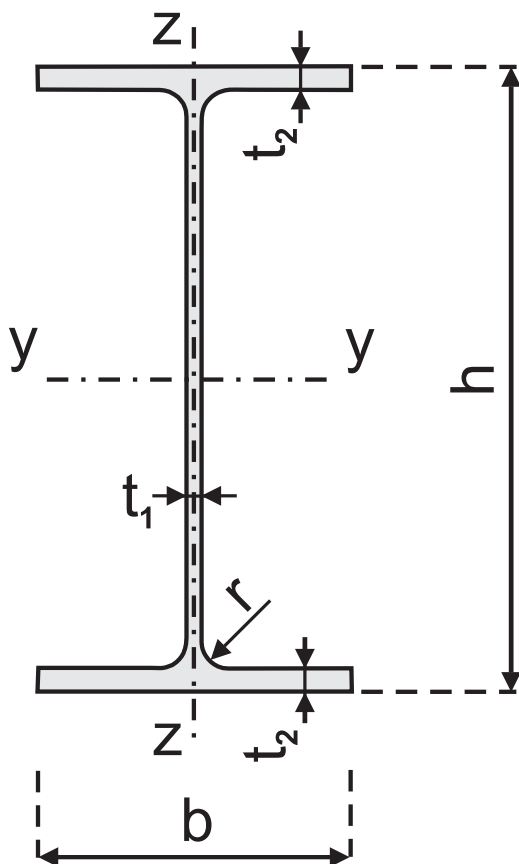
2. Lateral-torsional buckling of straight beams

The first available theoretical work on LTB of solid rectangular beams was published by Michell [20] and Prandtl [21]. Their work was extended by Timoshenko [22,23] to include the effect of warping torsion in IPE-beams.

For an idealized perfectly straight elastic IPE-beam, there are no out-of-plane x-z deformations until the applied bending moment M reaches the critical value M_{cr} and the beam buckles by deflecting laterally and twisting, see Fig. 2. This case represents a simple configuration, and buckling analysis leads to a close-form solution [24].

The deflection v and twist angle φ of the buckled shape can be obtained from two differential equations:

$$EI_z \frac{\partial^2 v}{\partial x^2} + M_{cr}\varphi = 0 \tag{1}$$

$$EI_\omega \frac{\partial^3 \varphi}{\partial x^3} - GI_t \frac{\partial \varphi}{\partial x} + M_{cr}\frac{\partial v}{\partial x} = 0 \tag{2}$$

where E is Young's modulus of elasticity, G is shear modulus, I_z is the second moment of area about axis z, I_ω is warping section constant, and I_t is torsion constant. The solution of Eqs. (1) and (2) satisfying the boundary conditions at the supports

$$(v)_0 = (v)_L = 0, \quad \left(\frac{\partial^2 v}{\partial x^2}\right)_0 = \left(\frac{\partial^2 v}{\partial x^2}\right)_L = 0, \quad (\varphi)_0 = (\varphi)_L$$

$$= 0, \quad \left(\frac{\partial^2 \varphi}{\partial x^2}\right)_0 = \left(\frac{\partial^2 \varphi}{\partial x^2}\right)_L = 0 \tag{3}$$
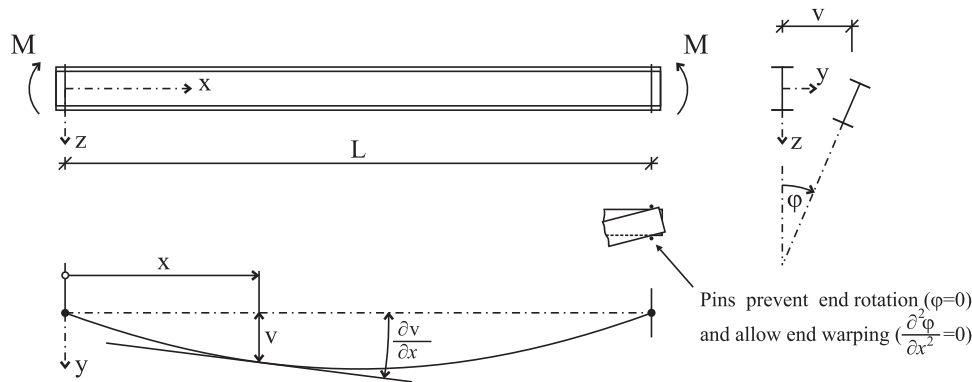

Fig. 1 – IPE cross-section.

Fig. 2 – Buckling of simply supported IPE-beam.

is given by the buckled shape with sinusoidal curvature

$$v = \frac{M_{cr}L^2}{\pi^2 EI_z}\varphi = a_{v,c}\sin\left(\frac{\pi x}{L}\right) \tag{4}$$

where $a_{v,c}$ is the indeterminate amplitude of deflection. Eq. (4) satisfies equilibrium equations (1) and (2) when

$$M_{cr} = \pi\frac{\sqrt{EI_z GI_t}}{L}\sqrt{1 + \frac{\pi^2 EI_\omega}{L^2 GI_t}} \tag{5}$$

This defines the elastic critical moment for LTB. The effect of the major axis curvature is neglected in Eq. (5).

3.   Deformation of beams with initial curvature and twist

The elastic deformation of simply supported beams with initial curvature v_0 and twist φ_0 caused by equal and opposite end bending moments M can be analyzed using the minor axis bending and torsion equations, see, e.g. [15].

$$EI_z\frac{\partial^2 v}{\partial x^2} + M(\varphi + \varphi_0) = 0 \tag{6}$$

$$EI_\omega\frac{\partial^3 \varphi}{\partial x^3} - GI_t\frac{\partial \varphi}{\partial x} + M\left(\frac{\partial v}{\partial x} + \frac{\partial v_0}{\partial x}\right) = 0 \tag{7}$$

The initial curvature v_0 and twist φ_0 were considered affine to the buckled shape (4) as a sine function.

$$\frac{v_0}{a_{v_0}} = \frac{\varphi_0}{a_{\varphi_0}} = \sin\left(\frac{\pi x}{L}\right) \tag{8}$$

where a_{v_0} and a_{φ_0} are amplitudes of initial deflection and twist. The solution of (6) and (7) satisfying boundary conditions (3) is given by

$$\frac{v}{a_v} = \frac{\varphi}{a_\varphi} = \sin\left(\frac{\pi x}{L}\right) \tag{9}$$

where a_v and a_φ are amplitudes of deflection v and twist φ of an imperfect beam loaded by bending moment M. If we differentiate Eq. (7) once and substitute into it from Eq. (6), we obtain

$$EI_\omega\frac{\partial^4 \varphi}{\partial x^4} - GI_t\frac{\partial^2 \varphi}{\partial x^2} - M^2\frac{\varphi + \varphi_0}{EI_z} + M\frac{\partial^2 v_0}{\partial x^2} = 0 \tag{10}$$

Substituting φ from (9) into (10) and v_0 and φ_0 from (8), we obtain

$$a_\varphi = \frac{M^2}{M_{cr}^2 - M^2}\left(a_{v_0}\frac{\pi^2 EI_z}{ML^2} + a_{\varphi_0}\right) \tag{11}$$

The initial curvature v_0 and twist φ_0 in (8) are identical in form to the buckled shape (4), thus with consideration to (8) and (4), we can write for amplitudes a_{v_0} and a_{φ_0}:

$$\frac{a_{v_0}}{a_{\varphi_0}} = \frac{M_{cr}L^2}{\pi^2 EI_z} \tag{12}$$

Substituting a_{v_0} from (12) into (11) and upon correction, we obtain Eq. (13).

$$\frac{a_\varphi}{a_{\varphi_0}} = \frac{M}{M_{cr} - M} \tag{13}$$

Using (8), (9), (12), (13) and upon substitution into (6), we obtain

$$\frac{a_v}{a_{v_0}} = \frac{M}{M_{cr} - M} \tag{14}$$

The longitudinal stress σ_x in the beam is the sum of the stresses due to the major axis bending, minor axis bending, and warping.

$$\sigma_x = \frac{M}{I_y}z - E\frac{\partial^2 v}{\partial x^2}y + E\frac{\partial^2 \varphi}{\partial x^2}\omega \tag{15}$$

where ω is the sectorial coordinate of the point. For the doubly symmetric IPE-beam depicted in Figs. 1 and 2, $\omega = -zy$. Eq. (15) may be rewritten using (9), (13), (14) as

$$\sigma_x = \frac{M}{I_y}z - E\frac{\partial^2 (v + z\varphi)}{\partial x^2}y$$
$$= \frac{M}{I_y}z + E(a_{v_0} + a_{\varphi_0}z)\frac{M}{M_{cr} - M}\frac{\pi^2}{L^2}\sin\left(\frac{\pi x}{L}\right)y \tag{16}$$

where I_y is the second moment of area about axis y. Substitution of (12) into (16) yields

$$\sigma_x = \frac{M}{I_y}z + a_{v_0}\frac{P_z}{I_z}\left(1 + \frac{P_z}{M_{cr}}z\right)\frac{M}{M_{cr} - M}\sin\left(\frac{\pi x}{L}\right)y \tag{17}$$

where $P_z = \pi^2 EI_z/L^2$. Extreme longitudinal stresses are at $x = L/2$, at the edges of flanges at $y = b/2$, $z = h/2$ (tension) and at $y = -b/2$,

$z = -h/2$ (compression). Maximum absolute values of longitudinal stress $\sigma_{x,max}$ are obtained from the equation

$$\sigma_{x,max} = \frac{M}{W_y} + |a_{v_0}| \frac{P_z}{W_z} \left(1 + \frac{P_z}{M_{cr}} \frac{h}{2}\right) \frac{M}{M_{cr} - M} \tag{18}$$

where $W_y = 2I_y/h$ is elastic section modulus about axis y, and W_z is elastic section modulus about axis z. The absolute value of a_{v_0} is considered in (18) so that input values of a_{v_0} may generally be positive and negative values, see Table 1. Let us denote the maximum elastic value of M as the elastic load carrying capacity M_R. If elastic limit is taken as the yield strength f_y, then M_R can be evaluated from the equation

$$\frac{M_R}{W_y} + |a_{v_0}| \frac{P_z}{W_z} \left(1 + \frac{P_z}{M_{cr}} \frac{h}{2}\right) \frac{M_R}{M_{cr} - M_R} = f_y \Rightarrow M_R \tag{19}$$

The solution of (19) yields the close-form equation (20) for the elastic load carrying capacity M_R [16].

$$M_R = -\frac{\sqrt{\left(4Q_1^2 + 4Q_1(Q_4 - 2M_{cr}Q_3) + Q_4^2 + 4M_{cr}Q_4Q_2 + 4M_{cr}^2Q_2^2\right)}}{4M_{cr}W_z}$$
$$+ \frac{2Q_1 + Q_4 + 2M_{cr}Q_2}{4M_{cr}W_z} \tag{20}$$

where

$$\begin{aligned} Q_1 &= f_y M_{cr} W_y W_z \\ Q_2 &= M_{cr} W_z + P_z |a_{v0}| W_y \\ Q_3 &= M_{cr} W_z - P_z |a_{v0}| W_y \\ Q_4 &= h P_z^2 |a_{v0}| W_y \end{aligned} \tag{21}$$

4.   Modelling of random imperfections

The load carrying capacity of a hot-rolled steel IPE-beam is generally a random variable, which is a function of random geometric and material characteristics. Stochastic analysis of the load carrying capacity can be performed on the computer using Monte Carlo based virtual simulations. The evaluation of M_R using the close-form equation (20) is fast and thus suitable for sampling based SA methods, which require repeated evaluation of M_R.

The profile IPE 220 chosen for the present study has been used extensively in previous reliability studies [8,10] of structural ultimate limit state. Geometric characteristics depicted in Fig. 1 are random variables obtained from results of experimental research [25], apart from the radius of curvature r, which was not measured. It was assumed that random variable r had mean value equal to the characteristic value of 12 mm. The variation coefficient r was considered the same as the value of the flange as 0.046, i.e. standard deviation is 0.552 mm.

Initial geometrical imperfections were assumed to follow the shape of the first eigenmode pertaining to LTB. The Gauss probability density function with mean value of zero (perfectly straight beam) was considered for the amplitude of initial curvature e_0. Standard deviation of the amplitude of initial curvature e_0 was evaluated based on the assumption that 95% of the realizations of e_0 were found within the tolerance limits $\pm L/1000$ [26,27]. The standard deviation e_0 obtained in such a manner is slightly lower than it was used in studies [10,17]. Both initial deflection a_{v_0} and rotation a_{φ_0} were considered. According to [26], we can write that

$$e_0 = a_{v0} + \frac{h}{2} a_{\varphi_0} \tag{22}$$

The relationship between a_{v_0}, a_{φ_0} and e_0 is depicted in Fig. 3.

Upon substitution from (12) into (22), we obtain

$$a_{v_0} = \frac{e_0}{1 + (h/2)(P_z/M_{cr})} \tag{23}$$

The statistical characteristics of Young's modulus E are considered according to two independently performed experimental researches [28]. The statistical characteristics of Poisson's ratio are considered according to [29]. The third variable characterizing material physico-mechanical properties is shear modulus of elasticity, which is calculated from the following equation

$$G = \frac{E}{2(1 + \mu)} \tag{24}$$

The histogram and statistical characteristics of yield strength of steel grade S235 were considered according to [9], where the results of tensile tests of samples obtained from a third of flanges of profiles IPE 160 to IPE 220 were published. Residual stress was not considered. All input random variables are clearly listed in Table 1. Truncated Gauss probability density functions were considered for variables r, E, μ so as to eliminate the negative values. Statistical correlations between input random variables are considered as null.

| Table 1 – Input random quantities.				
Symbol	Value	Density	Mean	Standard deviation
h	Cross-section height	Histogram	220.22 mm	0.975 mm
b	Flange width	Histogram	111.49 mm	1.093 mm
t_1	Web thickness	Histogram	6.225 mm	0.247 mm
t_2	Flange thickness	Histogram	9.136 mm	0.421 mm
r	Radius of curvature	Gauss	12 mm	0.552 mm
e_0	Initial imperfection	Gauss	0 m	L/1960
E	Modulus of elasticity	Gauss	210 GPa	10 GPa
μ	Poisson's ratio	Gauss	0.3	0.009
f_y	Yield strength	Histogram	297.3 MPa	16.8 MPa
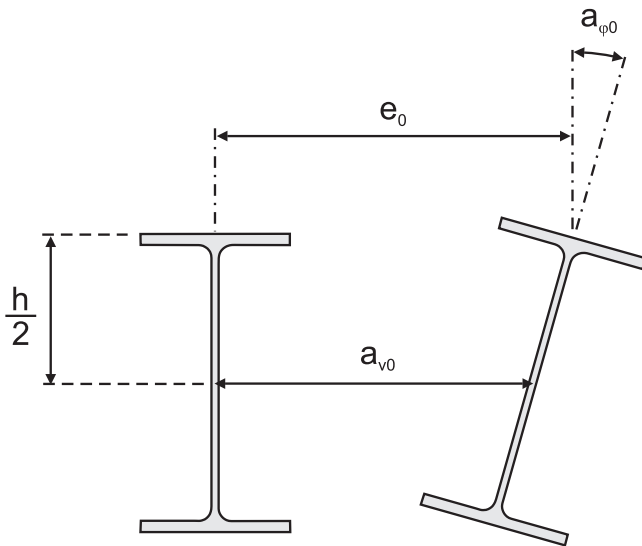
Fig. 3 – Amplitudes of initial deflections e_0, a_{v_0} and rotation a_{φ_0}.

The sectional characteristics are functions of the geometrical characteristics of the profile IPE illustrated in Fig. 1. It can be noted that profile IPE 220, whose geometric characteristics are listed in Table 1, is not a wide-flange beam. The profile IPE illustrated in Fig. 1 can be divided into rectangles and four rounded corners. The second moments of area I_y and I_z are evaluated from the equations:

$$I_y = \frac{1}{12}bh^3 - \frac{1}{12}(b - t_1)(h - 2t_2)^3 + 0.03r^4 + r^2(4 - \pi)\left(\frac{h}{2} - t_2 - r\frac{3\pi - 10}{3(\pi - 4)}\right)^2 \tag{25}$$

$$I_z = \frac{1}{6}t_2b^3 + \frac{1}{12}(h - 2t_2)t_1^3 + 0.03r^4 + r^2(4 - \pi)\left(\frac{t_1}{2} + r\frac{3\pi - 10}{3(\pi - 4)}\right)^2 \tag{26}$$

The torsion constant I_t is approximately given by the equation

$$I_t \approx \frac{1.28}{3}(2bt_2^3 + (h - 2t_2)t_1^3) \tag{27}$$

For equal flange IPE-beam

$$I_\omega = I_z\frac{(h - t_2)^2}{4} \tag{28}$$

5. Statistical analysis of elastic load carrying capacity

The statistical analysis was performed using the Latin Hypercube Sampling method (LHS); it is an improved variant of the Monte Carlo method [30,31]. LHS method was used to simulate 100 thousand runs of input random imperfections from Table 1. The output random variable is M_R (20). Simulation runs of M_R of the beam of length $L = 2.85$ m are depicted in Fig. 4. Results were depicted using the non-dimensional slenderness $\overline{\lambda}_{LT}$ [12]. The length $L = 2.85$ m corresponds to non-dimensional slenderness
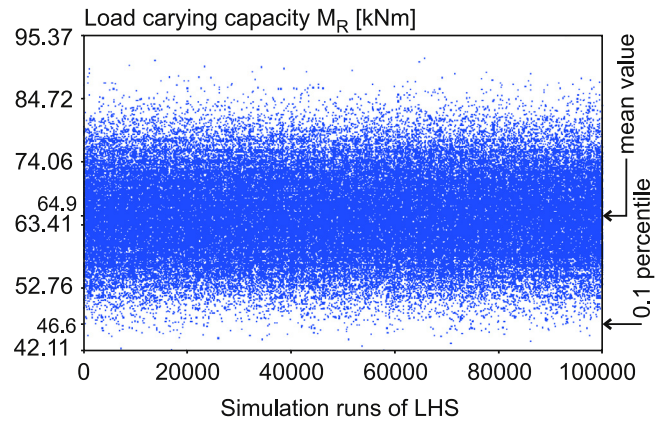

Fig. 4 – Statistical analysis M_R for $\overline{\lambda}_{LT} = 0.9$ ($L = 2.85$ m).

$\overline{\lambda}_{LT} = 0.9$, which was evaluated according to [12] from the equation

$$\overline{\lambda}_{LT} = \sqrt{\frac{W_{pl,y}\,f_{y,n}}{M_{cr,n}}} = \sqrt{\frac{67069}{M_{cr,n}}} \tag{29}$$

where $W_{pl,y} = 285.4 \times 10^3$ mm^3 is the nominal plastic section modulus about axis y of profile IPE220, $f_{y,n} = 235$ MPa is the nominal value of yield strength, and $M_{cr,n}$ is the elastic critical moment (5), which is a function of L and the nominal geometric and material characteristics according to [12]. Practically, the procedure is such that a value of $\overline{\lambda}_{LT}$ is chosen and the corresponding beam length L is evaluated from Eq. (29). Pairs ($\overline{\lambda}_{LT} = 1.0$, $L = 3.31$ m), ($\overline{\lambda}_{LT} = 1.1$, $L = 3.82$ m), etc. were obtained in this manner.

The mean value $M_{R,m} = 64.9$ kNm and design value $M_{R,0.1} = 46.6$ kNm calculated according to [11] as 0.1 percentiles are depicted in Fig. 4. The design value $M_{R,0.1}$ is lower (safer) than the mean value $M_{R,m}$. Value $M_{R,0.1}$ was evaluated from the fundamental definition of probability in such a way that 100 random realizations had a value lower than 46.6 kNm. The procedure for the calculation of 0.1 percentile was described in detail in [25].

The results of the statistical analysis of M_R depicted in Fig. 5 were evaluated for parameter $\overline{\lambda}_{LT}$ using the step-by-step
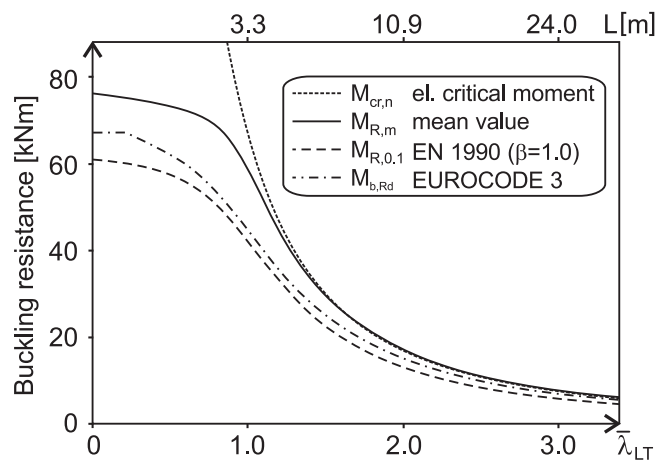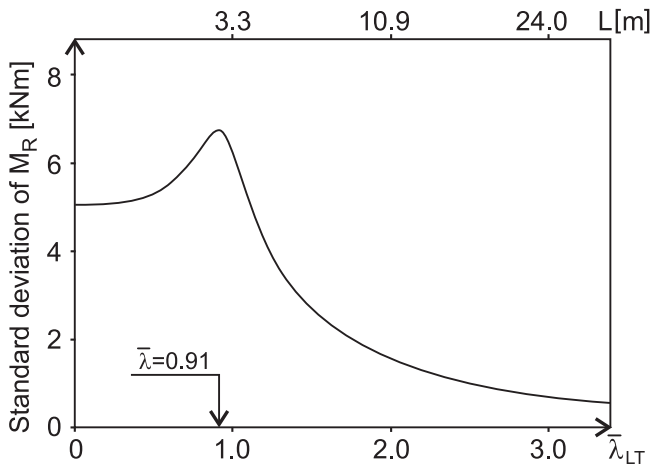

Fig. 5 – Statistical analysis of M_R.

Fig. 6 – Standard deviation of M_R vs $\overline{\lambda}_{LT}$.

method with the step of 0.01. The statistical analysis of M_R was evaluated for one million simulation runs of the LHS method for fixed value $\overline{\lambda}_{LT}$. For the sake of comparison, the design buckling resistance moment denoted in [12] as $M_{b,Rd}$ is depicted as well. Similar to its handling of column buckling [12] uses the Perry–Robertson formula for the characterization of beam LTB. The results of statistical analysis indicate reduced reliability of design according to [12] for relatively slender beams. It is apparent from Fig. 5 that if $\overline{\lambda}_{LT} < 1.5$, then $M_{R,0.1} < M_{b,Rd} < M_{R,m} < M_{cr,n}$. If $1.5 < \overline{\lambda}_{LT} < 20$, then $M_{R,0.1} < M_{b,Rd} < M_{cr,n} < M_{R,m}$. If $1.5 < \overline{\lambda}_{LT}$, then $M_{cr,n}/M_{R,0.1} \approx 1.3$. If $\overline{\lambda}_{LT} = 2$, then $M_{cr,n}/M_{b,Rd} \approx 1.12$, and if $\overline{\lambda}_{LT} < 2$, then $1.12 < M_{cr,n}/M_{b,Rd}$. The most dangerous ratio $M_{cr,n}/M_{b,Rd} \approx 1.011$ was found for $\overline{\lambda}_{LT} = 18$, it is not alarming, because beams with very high slenderness are not practically used in engineering practice. These conclusions are relevant mainly for slender beams; the reliability analysis of short beams will be supplemented in Section 7.

The decrease of $M_{R,0.1}$ in contrast to $M_{R,m}$ is most influenced by the standard deviation of M_R, see Fig. 6. The maximum value of standard deviation occurs for $\overline{\lambda}_{LT} = 0.91$. It is interesting to note that if $\overline{\lambda}_{LT} > 3$, then the variation coefficient value of M_R is approximately constant – 0.092.

6. Sensitivity analysis of elastic load carrying capacity

SA of a model output aims to quantify the relative importance of each model input parameter in the determination of the value of an assigned output variable [32]. Within the scope of modelling, the notion of ''sensitivity analysis'' has different meaning to different people, see, e.g. [18,33–35]. Regarding building structures, SA is an important part of the reliability analysis of concrete structures [36], masonry systems [37], and geotechnical structures [38]. For the identification of important parameters in models of steel structures, SA was applied, e.g. in [39–42].

Generally, there are two types of SA: local SA and global SA [18]. Local SA puts emphasis on the local (point) impact of input factors on the model output; local SA involves partial

derivatives (analytical or numerical). The local SA is practicable when the variation around the midpoint of input factors is small. Global SA focuses on the output uncertainty over the entire range of values of input parameters [32].

The influence of input random quantities X_i in Table 1 on the output M_R (20) should be studied by means of global SA. The presented paper deals with global Sobol's SA [43,44], which can be used for the non-linear function (20) with statistical independent input quantities having any type of distribution. Sobol's SA of M_R (20) is flexible, accurate and informative, and can be performed at reasonable computational cost. The main breakthrough in [43] is the computation algorithm that allows a direct estimation of global sensitivity indices using values of model output $Y(M_R)$ only [44]. Sobol first order sensitivity indices may be written in the form:

$$S_i = \frac{V(E(Y|X_i))}{V(Y)} \tag{30}$$

S_i measures the first order (e.g. additive) effect of X_i on the model output Y (M_R). The second order sensitivity index S_{ij} is the interaction term (31) between factors X_i, X_j. It captures that part of the response of Y to X_i, X_j that cannot be written as a superposition of effects separately due to X_i and X_j.

$$S_{ij} = \frac{V(E(Y|X_i, X_j))}{V(Y)} - S_i - S_j \tag{31}$$

Other Sobol sensitivity indices enabling the quantification of higher order interactions may be expressed similarly.

$$\sum_i S_i + \sum_i \sum_{j>i} S_{ij} + \sum_i \sum_{j>i} \sum_{k>j} S_{ijk} + \cdots + S_{123...M} = 1 \tag{32}$$

The number of members in (32) is $2^M - 1$, i.e. for $M = 3$, we obtain 7 sensitivity indices S_1, S_2, S_3, S_{12}, S_{23}, S_{13}, S_{123}; for $M = 9$, we obtain 511 sensitivity indices, which is excessively large for practical usage. The main limitation in the determination of all members of (32) is the computational demand.

Sensitivity indices were evaluated applying the LHS method. The conditional random arithmetical mean $E(Y|X_i)$ was evaluated for 100 000 simulation runs; the variance $V(E(Y|X_i))$ was calculated for 100 000 simulation runs as well. The variance $V(Y)$ of M_R is calculated on the assumption that all input imperfections are considered to be random ones; 1 000 000 runs were applied as well.

The results of Sobol's SA in Fig. 7 evaluated for $\overline{\lambda}_{LT} = 0.93$ ($L = 2.99$ m) show that Sobol's SA ranks the initial imperfection e_0 as the most important imperfection in determining M_R. For illustration, the random dependence between e_0 and M_R is depicted in Fig. 8. For beams with $\overline{\lambda}_{LT} = 0.93$, it may be noted that, if the standard deviation of e_0 is increased by 50%, then the value of $M_{R,0.1}$ decreases by 9%. Further significant imperfections include t_2 and f_y, whilst h, b, t_1, E have relatively low influence, see Fig. 7. The difference $1 - \sum_i S_i \approx 0.005$ in Fig. 7 shows that stochastic interactions in the model (20) are very small. Imperfections μ and r with first-order sensitivity indices approximately equal to zero may be considered as deterministic (non-random) variables having no effect on the variability of M_R. Practically, the deviation of M_R may be significantly reduced by decreasing the variability of e_0, e.g. by implementing stricter tolerance limits in production. The deviation of M_R decreases the most, if e_0 is considered as a deterministic (non-random) value.
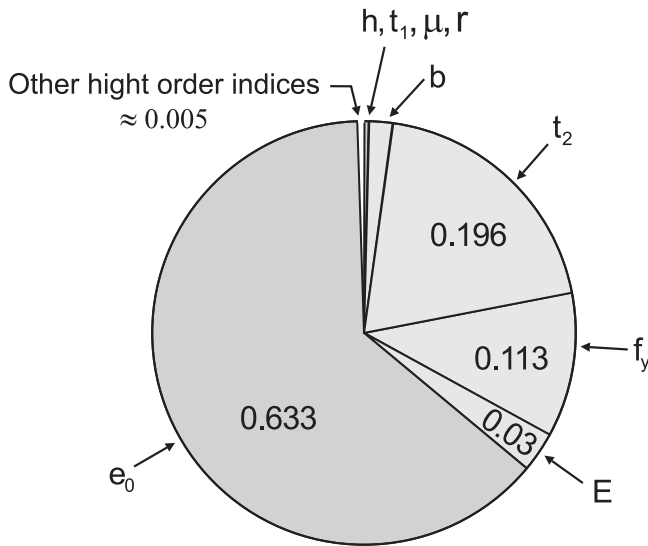
Fig. 7 – Sobol's SA for $\overline{\lambda}_{LT} = 0.93$.

Figs. 9 and 10 show box-whisker plots graphically depicting groups of numerical data through its seven numbers: sample minimum, one standard deviation below the mean value, lower quartile, median, upper quartile, one standard deviation above the mean value, and sample maximum. Each graph was evaluated using 100 000 simulation runs of the LHS method. In Fig. 9, the first graph from the left depicts the statistics of M_R evaluated assuming that all variables listed in Table 1 are considered as random variables. For the other graphs in Fig. 9, statistics of M_R have been evaluated assuming that all variables in Table 1 are considered as random, apart from the fixed (constant) variable listed under the graph. Fig. 10 depicts statistics of M_R evaluated for ten fixed values e_0. It is apparent from Figs. 9 and 10 that the random variability M_R (box height) decreases the most by fixing (freezing) e_0. It is clear from Fig. 10 that all seven monitored statistical characteristics decrease with increasing value of constant e_0.

The results of Sobol's SA depicted in Fig. 11 were evaluated for parameter $\overline{\lambda}_{LT}$ using the step-by-step method with the step
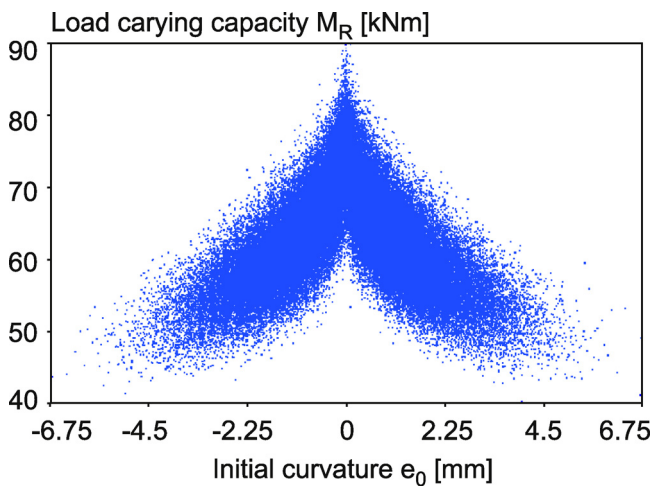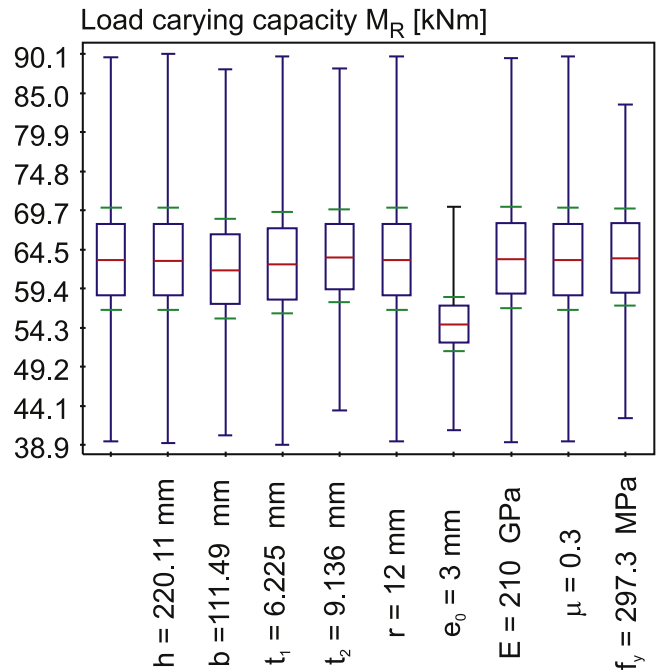

Fig. 9 – Box-whisker plots for $\overline{\lambda}_{LT} = 0.93$.

of 0.01. Imperfections f_y, e_0, t_2 deserve increased attention. For $\overline{\lambda}_{LT} < 0.71$, the variability of f_y has the greatest influence on the variability of M_R. On the contrary, for $\overline{\lambda}_{LT} > 1.0$ the variability of M_R is practically not influenced by the variability of f_y. If $\overline{\lambda}_{LT} > 1.13$, then t_2 is the dominant variable, otherwise t_2 is the second dominant variable. The second dominant variable for $\overline{\lambda}_{LT} > 1.13$ is Young's modulus E the variability of which cannot be practically influenced in production. The difference $1 - \sum_i S_i = 0.012$ shows that the higher order interactions between input variables in Table 1 are practically negligible in the model (20).
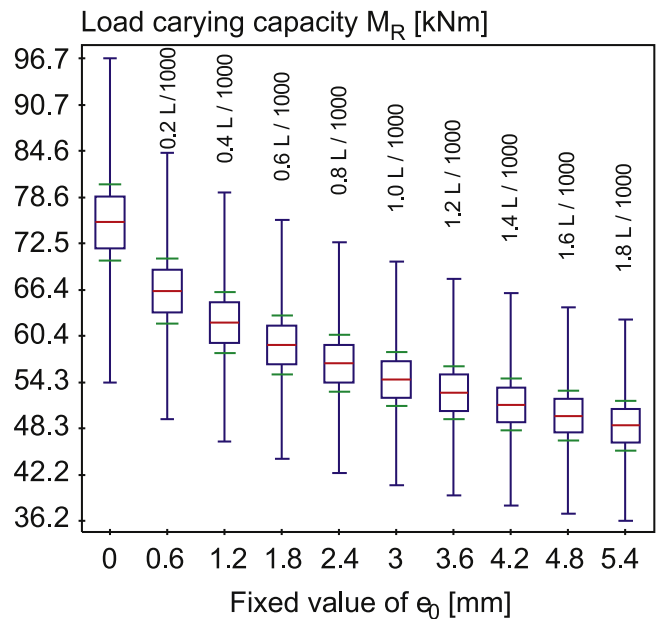

Fig. 8 – Random dependence between e_0 and M_R for $\overline{\lambda} = 0.93$.

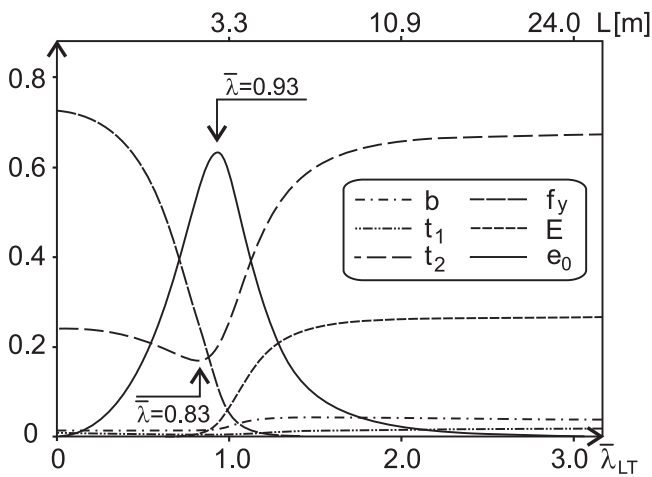Fig. 10 – Box-whisker plots for $\overline{\lambda}_{LT} = 0.93$.

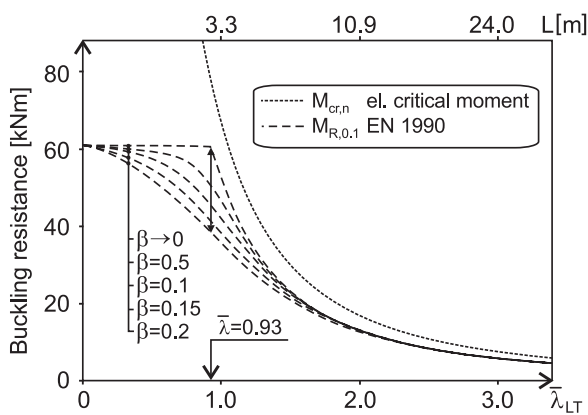Fig. 11 – Sobol indices S_i vs $\overline{\lambda}_{LT}$.

Fig. 12 – Statistical analysis of M_R for varying values of β.

For $0.71 \leq \overline{\lambda}_{LT} \leq 1.13$, M_R is most sensitive to the variability of e_0. This can be clearly illustrated by the following study. Let us consider the standard deviation of e_0 as $\beta L/1960$ and repeat the study, the results of which are depicted in Fig. 5. The results depicted in Fig. 12 clearly show the effect of the size of the standard deviation of e_0 (coefficient β) on design value $M_{R,0.1}$. The value of $M_{R,0.1}$ is most influenced by β for $\overline{\lambda}_{LT} = 0.93$, see Fig. 12. For $\beta \to 0$ ($e_0 \to 0$), we can notice that $M_{R,0.1}$ is smaller than $M_{cr,n}$, because the value of $M_{R,0.1}$ is influenced by the variability of other imperfections from Table 1. With the exception of results depicted in Fig. 12, $\beta = 1.0$ was considered in the rest of the article.

7.   Statistical analysis of inelastic load carrying capacity

The inelastic load carrying capacity can be determined by specifying some type of empirical curve, which gives essentially the elastic solution (20), and which terminates at the plastic moment capacity for short (or fully braced) beams. Some approximate relations and approaches suitable for finding close-form solutions to this problem are listed, e.g.
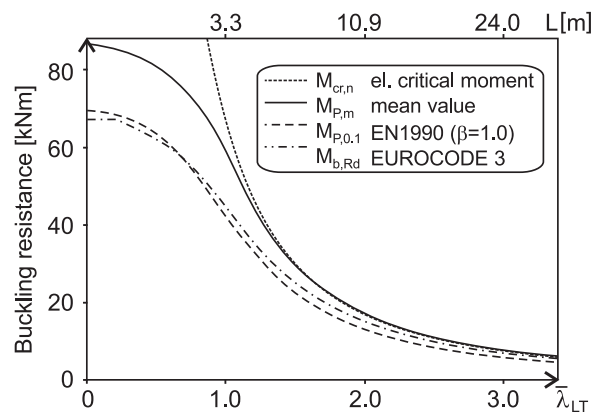

Fig. 13 – Statistical analysis of inelastic buckling resistance M_P.

in [45,46]. The inelastic load carrying capacity M_P was evaluated according to [17] as:

$$M_P = M_R \frac{W_{y,pl}}{W_y} \alpha + M_R(1 - \alpha) \qquad (33)$$

$W_{y,pl}$ is the inelastic section modulus about axis y. Variables M_P, $W_{y,pl}$, W_y in Eq. (33) are random and dependent on the random variability of variables in Table 1. α is a deterministic parameter considered according to [17] as

$$\alpha = \left(\frac{1}{1 + \overline{\lambda}_{LT}^4}\right)^4 \qquad (34)$$

Statistical analysis of M_P was performed for one million simulation runs of LHS method. Design value $M_{P,0.1}$ was evaluated according to [11] as 0.1 percentile. Reliability of design according to [12] may, in the basic form, be verified by the analysis $M_{P,0.1}$ vs λ_{LT}, see Fig. 13.

For a beam with $\overline{\lambda}_{LT} = 0$, we can note that $M_{P,0.1} = 69.5$ kNm. This value is 3% higher than $M_{b,Rd} = 67.1$ kNm according to [12], see Fig. 13. It is apparent from the comparison of Fig. 13 and Fig. 5 that results of statistical analyses are practically identical ($M_{R,m} \approx M_{P,m}$ and $M_{R,0.1} \approx M_{P,0.1}$) for slender beams with approximately $\overline{\lambda}_{LT} \geq 0.9$. It can be further noted that $M_{b,Rd}$ is higher (less safe) than $M_{P,0.1}$ for $\overline{\lambda}_{LT} \geq 0.7$, see Fig. 13. This indicates lower safety of design of slender beams according to [12]. The results of the statistical analyses complement the results of probabilistic analyses from [17], which showed a relatively high probability of failure (little safety) of very slender members designed according to [12].

8.   Conclusion

The reliability of load bearing beams may be increased in production primarily by decreasing the variability of initial material and geometrical imperfections. This can be practically achieved by setting appropriate tolerance limits of metallurgical standards and by increased control during production.

Results of SA of the elastic load carrying capacity M_R presented in this article have shown that the safety of bent IPE-beams may be significantly increased by decreasing the random variability of variables f_y, e_0, t_2, see Fig. 11.

- M_R is significantly influenced by the variability of yield strength f_y for $\overline{\lambda}_{LT} < 0.71$. If $\overline{\lambda}_{LT} = 0$, then it is a simple bending task, where the load carrying capacity is dependent solely on the magnitude of yield strength and the geometry of the cross section. For $\overline{\lambda}_{LT} = 0$ the sensitivity coefficient of yield strength is $S_{f_y} = 0.73$, and since the higher order interactions are very small the sum of sensitivity coefficients of variables h, b, t_1, t_2, r can be considered as approximately $1 - 0.73 = 0.27$, of which the flange thickness has the dominant influence $S_{t_2} = 0.24$ (variability of b, t_1, r can be neglected), see Fig. 11.

- M_R is significantly influenced by the variability of e_0 if $0.71 \leq \overline{\lambda}_{LT} \leq 1.13$. M_R is most sensitive to e_0 for $\overline{\lambda}_{LT} = 0.93$. The maximum value of the standard deviation of M_R was obtained for $\overline{\lambda}_{LT} = 0.91$, see Fig. 6. Beams with slenderness around 0.9 occur very frequently in structural systems; therefore it is necessary to pay increased attention to random variable e_0. We should strive for minimal values of e_0 (straight beams).

- M_R is most sensitive to the variability of t_2 if $\overline{\lambda}_{LT} > 1.13$, otherwise t_2 is the second dominant variable. If $\overline{\lambda}_{LT} > 1.28$ then the second dominant variable is Young's modulus E.

In probabilistic assessments of reliability, imperfections f_y, e_0, t_2 belong to the crucial input random variables, whose variability should be determined through precise measurement. The reliability of the beam increases if the variability of parameters f_y, e_0, t_2 decreases. Reduction of the variability of flange thickness t_2 can generally be recommended for all slenderness values, see Fig. 11. It may be noted that while the statistical characteristics of imperfections f_y, t_2 have long been studied by experimental research [9,25], standard deviation of the amplitude of initial curvature e_0 is discussed in connection with aleatory and also epistemic (fuzzy) uncertainties [10].

Let us now compare the SA results in this article with the results of SA [19] examining the effects of initial imperfections on the load carrying capacity R of a steel member under compression. Non-dimensional slenderness $\overline{\lambda}_{LT}$ and $\overline{\lambda}$ implemented as analysis parameters enable approximate comparison of SA results of two different stability problems. The comparison of results in Fig. 11 and Fig. 2 in [19] shows that the effect of variability of t_2 on M_R (bending) is higher than the effect of variability of t_2 on R (compression), especially for higher slenderness values. The effect of the variability of t_2 on M_R is dominant for $\overline{\lambda}_{LT} > 1.13$, see Fig. 11. The effect of e_0 on M_R is slightly different than the effect of e_0 on R [19]. Sensitivity index S_{e_0} describing the main effect of e_0 on M_R decreases very rapidly if $\overline{\lambda}_{LT} > 0.93$ and is practically null if $\overline{\lambda}_{LT} > 2.0$, see Fig. 11. On the contrary, S_{e_0} describing the main effect of e_0 on R decreases relatively slower, e.g. for $\overline{\lambda} = 2.0$, $S_{e_0} = 0.22$ [19].

The difference $1 - \sum_i S_i \approx 0$ shows that the higher order interactions effects [18] between input imperfections are practically negligible in the model (20). A similar conclusion was reached in [19]. Practically, this means that M_R and R can be approximated, in stochastic models, by additive models that neglect these interactions.

Statistical analysis shows that for $\overline{\lambda}_{LT} < 0.7$ design resistance, $M_{b,Rd}$ evaluated according to [12] is lower (safer) than the value $M_{P,0.1}$, see Fig. 13. On the contrary if $\overline{\lambda}_{LT} \geq 0.7$, then $M_{R,0.1} < M_{P,0.1} < M_{b,Rd}$, which suggests smaller design reliability according to [12]. Reliability of IPE-beams with $\overline{\lambda}_{LT} \geq 0.7$ can be increased by decreasing the random variability of imperfections e_0, t_2, which have a large influence on M_R.

The design of very slender beams $\overline{\lambda}_{LT} \geq 1.5$ is relatively very unsafe. The design value $M_{R,0.1}$ obtained from the statistical analysis is significantly lower than the design value $M_{b,Rd}$ according to [12] for slender beams. The standard [12] considers the design buckling resistance moment $M_{b,Rd}$ of slender beams dangerously close to the elastic critical moment $M_{cr,n}$. With the aim of ensuring a more safe design, standard values $M_{b,Rd}$ should be lower for very slender beams. This could be achieved by increasing the values of partial safety factors or the calibration of lateral-torsional buckling curves. As illustrated by the sensitivity analysis results it is necessary to strive for the reduction of the random variability of imperfections, especially of the flange thickness t_2, for very slender IPE-beams. This can be achieved by increased control in production and the control of the hot-rolling process of these beams.

The reliability of hot-rolled IPE-beams can be influenced just a little by changing the mean values of initial imperfections, which in most cases, should be equal to their nominal values, see Table 1. An exception is the yield strength; its mean value is greater than the characteristic value. Standards and manufacturers guarantee minimum yield strength, which reflects 5% quantile of the actual probability density distribution. However, the average yield strength is not guaranteed by standards or by a manufacturer, and is based mainly on production technology.

Acknowledgements

REFERENCES

[1] T.V. Galambos, A.E. Surovek, Structural Stability of Steel: Concepts and Applications for Structural Engineers, John Wiley & Sons, New Jersey, 2008.

[2] J. Zahn, Lateral stability of beams with initial imperfections, Journal of Engineering Mechanics 109 (3) (1983) 821–835.

[3] H. Yoshida, K. Maegawa, Lateral instability of I-beams with imperfections, Journal of Structural Engineering 110 (8) (1984) 1875–1892.

[4] P. Marek, J. Brozzetti, M. Gustav, P. Tikalsky, Probabilistic Assessment of Structures using Monte Carlo Simulation, TeReCo, Prague, 2003.

[5] D. Schillinger, Stochastic FEM based stability analysis of I-sections with random imperfections, (Diploma Thesis), Stuttgart University, 20081–93.

[6] D. Schillinger, D. Stefanov, A. Stavrev, The method of separation for evolutionary spectral density estimation of multi-variate and multi-dimensional non-stationary stochastic processes, Probabilistic Engineering Mechanics 33 (2013) 58–78.

[7] S. Shayan, K. Rasmussen, H. Zhang, On the modelling of initial geometric imperfections of steel frames in advanced analysis, Journal of Constructional Steel Research (98) (2014) 167–177.

[8] Z. Kala, Geometrically non-linear finite element reliability analysis of steel plane frames with initial imperfections, Journal of Civil Engineering and Management 18 (1) (2012) 81–90.

[9] J. Melcher, Z. Kala, M. Holický, M. Fajkus, L. Rozlívka, Design characteristics of structural steels based on statistical analysis of metallurgical products, Journal of Construction Research 60 (3–5) (2004) 795–808.

[10] Z. Kala, Stability problems of steel structures in the presence of stochastic and fuzzy uncertainty, Thin Walled Structures 45 (10–11) (2007) 861–865.

[11] EN 1990, Eurocode-Basic of Structural Design, CEN, Brussels, 2002.

[12] EN 1993-1-1, Eurocode 3: Design of Steel Structures. Part 1-1. General Rules and Rules for Buildings, CEN, Brussels, 2004.

[13] G. Sedlacek, H. Stangenberg, Design philosophy of Eurocodes – background information, Journal of Constructional Steel Research 54 (1) (2000) 173–190.

[14] G. Sedlacek, Ch. Müller, The European standard family and its basis, Journal of Constructional Steel Research 62 (11) (2006) 1047–1059.

[15] N.S. Trahair, The Behaviour and Design of Steel Structures, John Wiley & Sons, New York, 1977.

[16] Z. Kala, Elastic lateral-torsional buckling of simply supported hot-rolled steel I-beams with random imperfections, Procedia Engineering 57 (2013) 504–514.

[17] Z. Kala, Reliability analysis of the lateral torsional buckling resistance and the ultimate limit state of steel beams with random imperfections, Journal of Civil Engineering and Management (2015), http://dx.doi.org/10.3846/13923730.2014.971130 (in press).

[18] A. Saltelli, K. Chan, E.M. Scott, Sensitivity Analysis, Wiley Series in Probability and Statistics, John Wiley & Sons, New York, 2004.

[19] Z. Kala, Sensitivity assessment of steel members under compression, Engineering Structures 31 (6) (2009) 1344–1348.

[20] A.G.M. Michell, Elastic stability of long beams under transverse forces, Philosophical Magazine 48 (1899) 298–309.

[21] L. Prandtl, Kipperscheinungen (PhD Dissertation), Munich, Germany, 1899.

[22] S.P. Timoshenko, Einige Stabilitätsprobleme der Elastizitätstheorie, Collected papers of Stephen P. Timoshenko, McGraw-Hill, New York, 19531–50.

[23] S.P. Timoshenko, Sur la stabilité des systèmes élastiques, Collected papers of Stephen P. Timoshenko, McGraw-Hill, New York, 195392–224.

[24] S.P. Timoshenko, J.M. Gere, Theory of Elastic Stability, 2nd ed., McGraw-Hill, New York, 1961.

[25] Z. Kala, J. Melcher, L. Puklický, Material and geometrical characteristics of structural steels based on statistical analysis of metallurgical products, Journal of Civil Engineering and Management 15 (3) (2009) 299–307.

[26] A. Taras, R. Greiner, New design curves for lateral-torsional buckling – proposal based on a consistent derivation, Journal of Constructional Steel Research 66 (5) (2010) 648–663.

[27] C. Rebelo, N. Lopes, L. Simões da Silva, D. Nethercot, P.M.M. Vila Real, Statistical evaluation of the lateral-torsional buckling resistance of steel I-beams. Part 1: Variability of the Eurocode 3 resistance model, Journal of Constructional Steel Research 65 (2009) 818–831.

[28] G.C. Soares, Uncertainty modelling in plate buckling, Structural Safety 5 (1) (1988) 17–34.

[29] JCSS, Probabilistic Model Code. Part 3 – Resistance Models, Joint Committee on Structural Safety, 2001 http://www.jcss.ethz.ch/.

[30] M.D. McKey, W.J. Conover, R.J. Beckman, A comparison of the three methods of selecting values of input variables in the analysis of output from a computer code, Technometrics 21 (2) (1979) 239–245.

[31] R.C. Iman, W.J. Conover, Small sample sensitivity analysis techniques for computer models with an application to risk assessment, Communications in Statistics – Theory and Methods 9 (17) (1980) 1749–1842.

[32] T. Homma, A. Saltelli, Importance measures in global sensitivity analysis of nonlinear models, Reliability Engineering & System Safety 52 (1) (1996) 1–17.

[33] D.G. Cacuci, Sensitivity and Uncertainty Analysis, vol. 1: Theory, Chapman and Hall/CRC Press, Boca Raton, FL, 2003.

[34] A. Yazdani-Chamzini, An integrated fuzzy multi criteria group decision making model for handling equipment selection, Journal of Civil Engineering and Management 20 (5) (2014) 660–673.

[35] A. Mardani, A. Jusoh, E.K. Zavadskas, Fuzzy multiple criteria decision-making techniques and applications – two decades review from 1994 to 2014, Expert Systems with Applications 42 (8) (2015) 4126–4148.

[36] I.H. Yang, Uncertainty and sensitivity analysis of time-dependent effects in concrete structures, Engineering Structures 29 (7) (2007) 1366–1374.

[37] R. Sousa, J. Guedes, H. Sousa, Characterization of the uniaxial compression behaviour of unreinforced masonry – sensitivity analysis based on a numerical and experimental approach, Archives of Civil and Mechanical Engineering 15 (2) (2015) 532–547.

[38] D. Marčić, A. Cerić, M.S. Kovačević, Selection of a field testing method for karst rock mass deformability by multi criteria decision analysis, Journal of Civil Engineering and Management 19 (2) (2013) 196–205.

[39] J. Gottvald, Z. Kala, Sensitivity analysis of tangential digging forces of the bucket wheel excavator SchRs 1320 for different terraces, Journal of Civil Engineering and Management 18 (5) (2012) 609–620.

[40] Z. Kala, J. Gottvald, J. Stoniš, A. Omishore, Sensitivity analysis of the stress state in shell courses of welded tanks for oil storage, Engineering Structures and Technologies 6 (1) (2014) 7–12.

[41] L. Cascini, F. Portioli, R. Landolfo, Probabilistic time variant assessment of thin-walled steel members under atmospheric corrosion attack, Journal of Civil Engineering and Management 20 (3) (2014) 404–414.

[42] M. Kamiński, P. Świta, Structural stability and reliability of the underground steel tanks with the stochastic finite element method, Archives of Civil and Mechanical Engineering 15 (2) (2015) 593–602.

[43] I.M. Sobol', Sensitivity estimates for nonlinear mathematical models, Mathematical Modelling and Computational Experiment 1 (4) (1993) 407–414 [Translated from Russian. Sobol', IM. Sensitivity estimates for nonlinear mathematical models. Matematicheskoe Modelirovanie 2 (1) (1990) 112–118].

[44] I.M. Sobol', Global sensitivity indices for nonlinear mathematical models and their Monte Carlo estimates, Mathematics and Computers in Simulation 55 (1–3) (2001) 271–280.

[45] T.V. Galambos, Guide to Stability Design Criteria for Metal Structures, Structural Stability Research Council, John Wiley & Sons, New York, 1998.

[46] R.D. Ziemian, Guide to Stability Design Criteria for Metal Structures, John Wiley & Sons, New Jersey, 2010.